Anisotropic Depth Migration Applied in an Area of the Colombian Llanos Foothills as a Key to Understanding the Structure in Depth

Rob Vestrum*, ***Thrust Belt Imaging, Calgary, Canada;***
Isabel Cristina Florez, ***Hocol S.A., Bogotá, Colombia;***
Jon Gittins, ***Thrust Belt Imaging, Calgary, Canada***

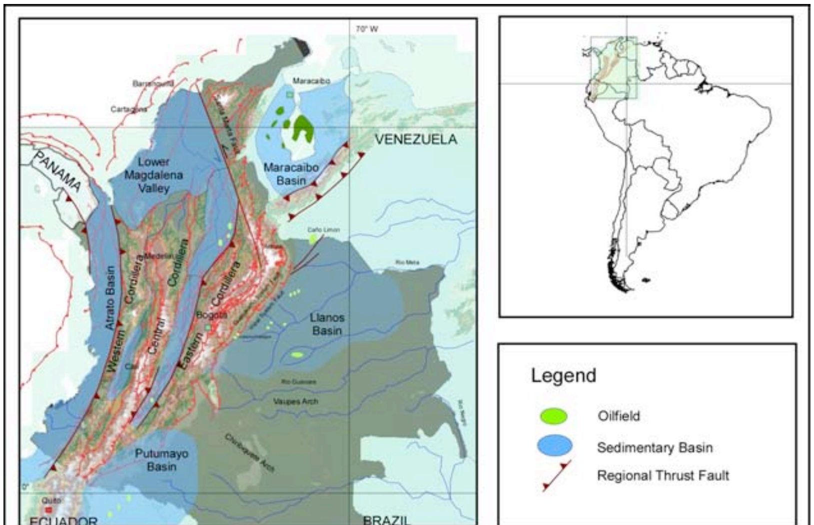

Figure 1. Map location

ABSTRACT

The objective of the depth imaging was to confirm the existence of the structure in depth, improving the image and obtaining more accurate positioning of the events for an appropriate well trajectory.

We used a collaborative, geologically constrained approach that integrates all available geologic information into the interpretation of the seismic velocity model. Close collaboration between the exploration geologist and the service-company geophysicist found a velocity model that optimized the seismic imaging. This area has interbedded siliciclastic rocks with high dips and vertical and lateral velocity contrasts, giving a considerable lateral movement in the images in depth when we correct for seismic anisotropy and lateral-velocity heterogeneity.

The final anisotropic-depth-migrated image confirms the structure and moves the imaged structured to the east compared to the time image. The position of the structure and dips were confirmed by two wells drilled in the area, which verifies the accuracy of the seismic-imaging algorithm and the interpretive model-building process in this complex-structured area.

INTRODUCTION

The foothills belt of the Eastern Cordillera has high-dipping siliciclastic rocks adjacent to the flatter lying beds in the western limit of the foreland Llanos basin (see Figure 1). This zone is characterized by lateral contrast and inversion of velocities in a complex setting of thrusts that lead to a change in the position of the events when migrating from time to depth.

We decided to perform a prestack anisotropic depth migration, which incorporates the anisotropic variables and dips in the processing. The goal was to challenge our structural model and obtain a lateral and vertical uncertainty range for the position of the target before drilling. We knew from studies of migration from time to depth of seismic interpretation in these areas that the amount of movement of the events can be a critical issue for the well planning due to the considerable magnitude of movement that we observed.

Figure 2 shows the shift one can expect on a subsurface structure below dipping anisotropic clastic rocks. The velocity parallel to the shale bedding is higher than the velocity perpendicular to bedding, so rays from the eastern or up-dip side of the structure will travel at a higher velocity than rays from the western or cross-dip side of the structure. The least-time raypath will have a longer travelpath in the higher-velocity direction, as shown by the yellow raypath in Figure 2. If we process these seismic data assuming isotropy, the imaged reflector will be in the wrong position.

The geometry of the subsurface, as shown in Figure 3, is more complicated than the simplified cross-section in Figure 2, which has a horizontal target below uniform 45°-dipping anisotropic strata. The model geometry shows laterally varying dip in anisotropic strata and lateral-velocity variation above the target reflector; we were not confident that we could accurately predict the lateral-movement of the structures from simple geometric arguments. Aside from the difficulty predicting lateral-position error on the subsurface targets, we predicted that correcting for anisotropic and lateral-velocity effects would improve the clarity of the imaged reflectors.

GEOLOGICAL SETTING

The Llanos foothills are located to the northeast of Bogotá city in the eastern flank of the Eastern Colombian Cordillera, near the edge of the Llanos Basin. The northern part of these Llanos foothills are characterized by a series of duplexes of low to moderate angle with west verging of thin-skin tectonics that shorten the stratigraphic section in about 40%. The stratigraphic sequence involved in duplexing goes from Lower Miocene down to Lower and Middle Cretaceous.

MODEL BUILDING METHOD

Seismic velocity changes with direction relative to the dip of the strata, therefore an accurate representation of the subsurface model dip is essential for an accurate anisotropic depth migration. We interpreted dip-direction and dip-magnitude volumes based on the orientation of the seismic reflectors and a correlation with dip-meter data.

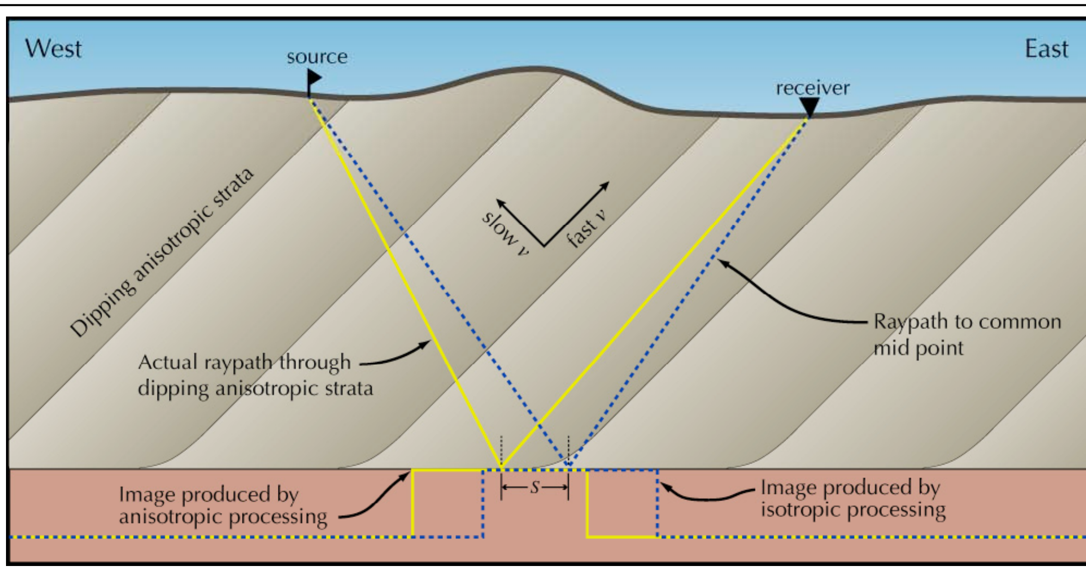

Figure 2. Cross-section showing lateral movement predicted from isotropic processing of data where transverse isotropy with a tilted axis of symmetry is present. The dashed lines represent the result of isotropic processing. *S* is the distance between the actual subsurface reflection point and the reflection point when the processing algorithm assumes isotropy (modified from Vestrum et al, 1999).

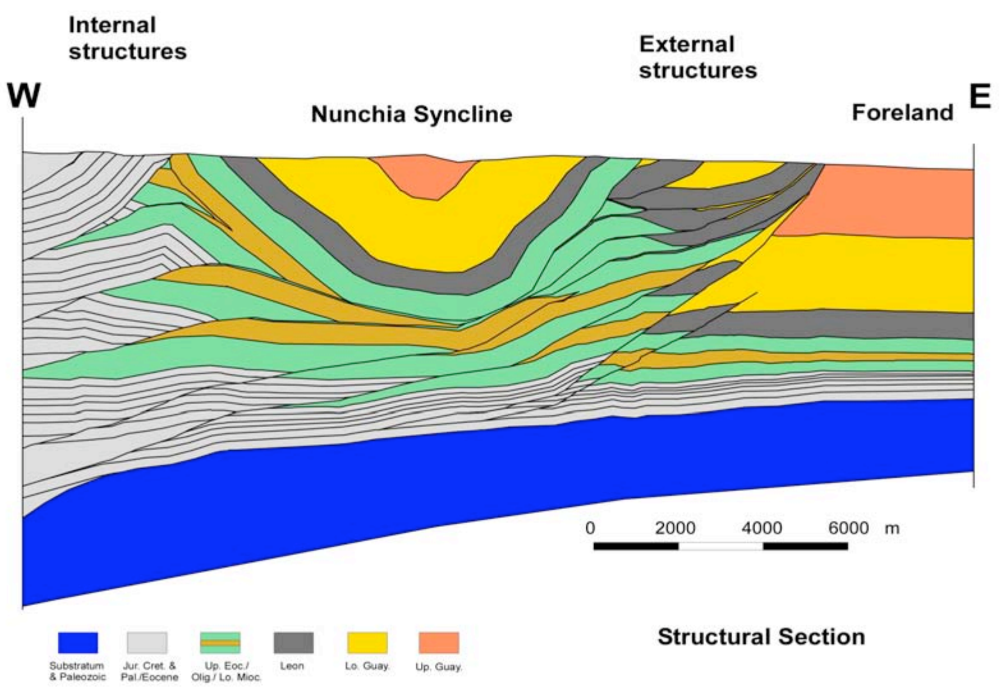

Figure 3. Schematic Structural Section: The foothills belt in the area can be separated into 4 areas as described with details by Rochat et al, 2003: Internal Structures in the western part, Nunchia Syncline that extends widely in the area and External Structures next to the western limit of the Foreland (figure from Rochat et al, 2003).

Starting with the initial interpretation, we populated our velocity model. By starting with nonzero values for our anisotropic parameters, in this case ε=12% and δ=3%, and an initial interpretation of the dip field from our structural interpretation, we avoided interpreting velocity updates that yield artificially high velocities because we have ignored the anisotropy in our clastic overburden. Anisotropy is a major factor in the mis-tie between seismic and well-log velocities (Schultz and Canales, 1997; Schultz, 1999). Even though our initial estimate of the anisotropy parameters may have been inaccurate, we found in past experience (e.g., Vestrum and Muenzer, 1997; Vestrum et al., 1999; Lawton et al., 2001; Vestrum, 2002; etc.) that moderate values for anisotropy parameters allowed us to create a depth-migrated volume with an optimum image that also yields accurate reflector depths.

Velocity updates employed traditional image-gather analysis (Zhu et al., 1998). We followed the manual-tomography methodology described by Murphy and Gray (1999). Where image-gather analysis was deficient, we used a basic trail-and-error approach where we tested different interpretations and evaluated the tests based on the changes in the depth-migrated image. We interpreted the velocity updates, being careful to have a geological justification for any velocity changes. We worked to keep the seismic model velocities close to the well velocities so that we maintained a tie between the well depths and the depths of correlated seismic events.

Figure 4 shows a screen capture of the interactive model-building display. The depth-migrated seismic data for the current model were overlaid on a colour map of the velocity model. The program raytraced the velocity model and applied velocity changes to the image gathers. The model interpreter selected the velocity perturbation that best flattened the image gathers.

RESULTS

The final depth image is shown in Figure 7. If we compare back to the original poststack-time-migrated volume used in the initial interpretation (Figure 5), we can see lateral-position changes on

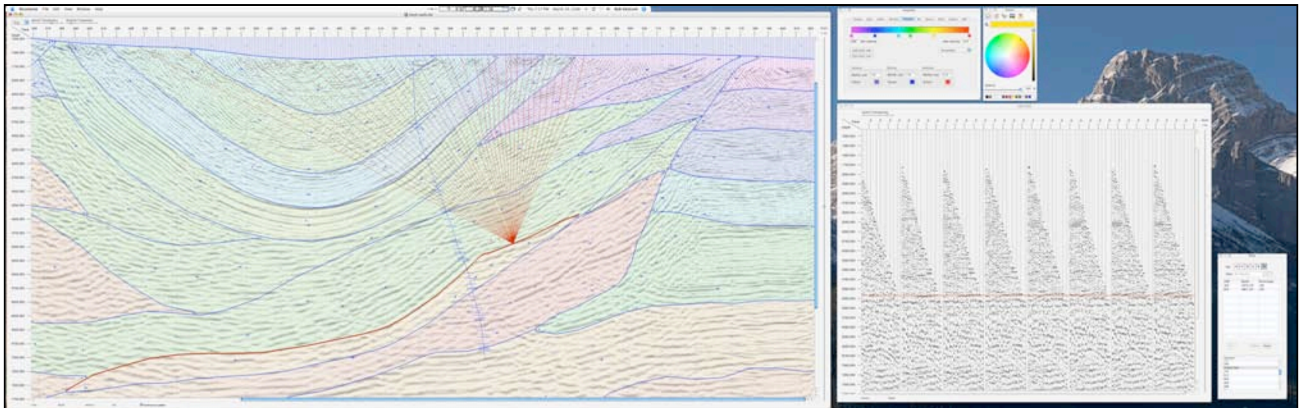

Figure 4. Interactive model-building display showing seismic data overlaid on the velocity model on the left and image-gather diagnostics in the window to the right.

the major features of the seismic data. The green marker on each if these figures (Figures 5, 6, and 7) shows the position that the well intersects the target horizon. The lateral-position difference between the time-migrated image (Figure 5) and the anisotropic depth-migrated image (Figure 7) at the target level results from the improvement in imaging that revealed more of the target horizon. The anisotropy and lateral-velocity heterogeneity in the strata above the target caused wave-propagation effects that limit the ability of time processing to image the leading edge of the target reflector.

The circles on the three seismic figures (Figures 5, 6, and 7) illustrate the change in vertical and horizontal position of the fold in the dipping reflector between the three imaging algorithms: (1) time migration, the most stable imaging algorithm, (2) isotropic depth migration, which corrects for lateral heterogeneity, and (3) anisotropic depth migration, which corrects for both heterogeneity and anisotropy. The yellow circle surrounds a fold imaged on the time section (Figure 5), the blue circle indicates the position of this same fold on the isotropic depth migration (Figure 6), and the red circle highlights the position of the fold on the anisotropic depth migration (Figure 7).

The lateral-position change from time to depth–from yellow to blue–is due to correcting for lateral heterogeneity. The shift from blue to red, with the additional correction for anisotropy, is to the left, which is the down-dip direction of the TTI layers above the fold. The TTI layers in Figure 2 have a similar left-dipping orientation, and this figure predicts that ignoring anisotropy results in the target imaged to the right of its true position, a prediction confirmed by Figures 6 and 7 with the image on the isotropic depth migration (blue) to the right of the anisotropic depth migration (red). Note also that the vertical position of the encircled feature is deeper on the isotropic depth migration because ignoring anisotropy requires a higher velocity than the true vertical velocity to produce a coherent image.

Going from time to isotropic depth, correcting for lateral heterogeneity moved the structure far to the right. Going from isotropic depth migration to anisotropic depth migration, the structure moved to the left, which matches the lateral shift predicted in Figure 2. The reflector intervals and depths on the anisotropic depth migration matched more closely to the well tops.

CONCLUSIONS

Prestack anisotropic depth migration is an additional tool that brings value to the seismic data, incorporating variables of the intrinsic rock properties to the image in depth. It offered the opportunity to visualize the structure in a more realistic position. The well results confirmed the accuracy of the leading edge of the structure, which was not imaged using previous processing methods.

Geologically constrained velocity-model interpretation enabled us to overcome the limitations in our seismic data to improve the image quality and accuracy of the imaged reflectors.

ACKNOWLEDGMENTS

We acknowledge Hocol and TBI for permission and support to publish this work. Thanks to Hocol staff who collaborated with the project: Luis Fernando Castaño, José Arturo Jaramillo, Alexis Rosero, Antonio Rocha, Henry Lara and specially Mario De Freitas for his valuable suggestions.

REFERENCES

Murphy, G. E. and Gray, S. H., 1999, Manual seismic reflection tomography: Geophysics, Soc. of Expl. Geophys., 64, 1546-1552.

Schultz, P., 1999, The Seismic Velocity Model as an Interpetation Asset: Soc. of Expl. Geophys.

Schultz, P. and Canales, L., 1997, Seismic velocity model building: CE in Dallas, 2 November: The Leading Edge 16, 1063-1064.

Thomsen, L., 1986, Weak elastic anisotropy: Geophysics, 51, 1954-1966.

Vestrum, R. W., 2002, 2D and 3D anisotropic depth migration case histories: 72nd Annual Internat. Mtg., Soc. Expl. Geophys.

Vestrum, R.W. and Muenzer, K., 1997, Imaging below dipping anisotropic shale: CSEG 1997 National Meeting.

Vestrum, R. W., Lawton, D.C., and Schmid, R. S., 1999, Imaging structures below dipping TI media: Geophysics, 64, no. 4, 1239-1246.

Zhu, J., Lines, L. and Gray, S., 1998, Smiles and frowns in migration/velocity analysis: Geophysics, Soc. of Expl. Geophys., 63, 1200-1209.

Lawton, D.C., Isaac, J.H., Vestrum, R.W., and Leslie, J.M., 2001, Slip slidin' away—some practical implications of seismic velocity anisotropy on depth imaging: The Leading Edge, 19, no. 1, 70-73.

Rochat, P., Rosero, A., Gonzales, R, Florez, I., Lozada, M. and Petton, R., 2003, Thrust kinematics of the Tangara/Mundonuevo Area: New Insight From Apatite Fission Track Análisis: VIII Simposio Bolivariano – Exploración Petrolera en las Cuencas Subandinas, 147-154.

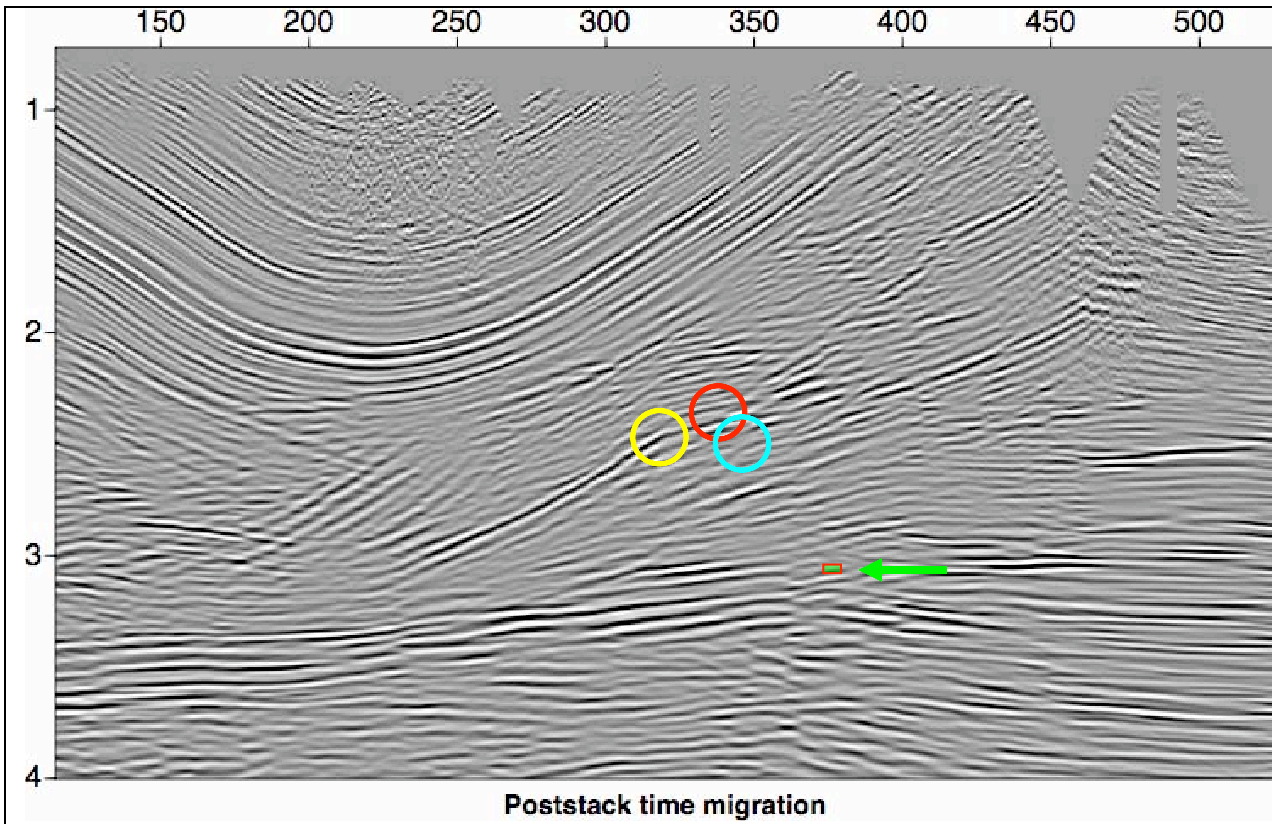

Figure 5. Inline slice from poststack time migration. The green marker represents the position that the well intersected the target horizon. The circles show the position of a fold on a reflector as it appears on the time section (yellow), the isotropic depth section (blue), and the anisotropic depth section (red).

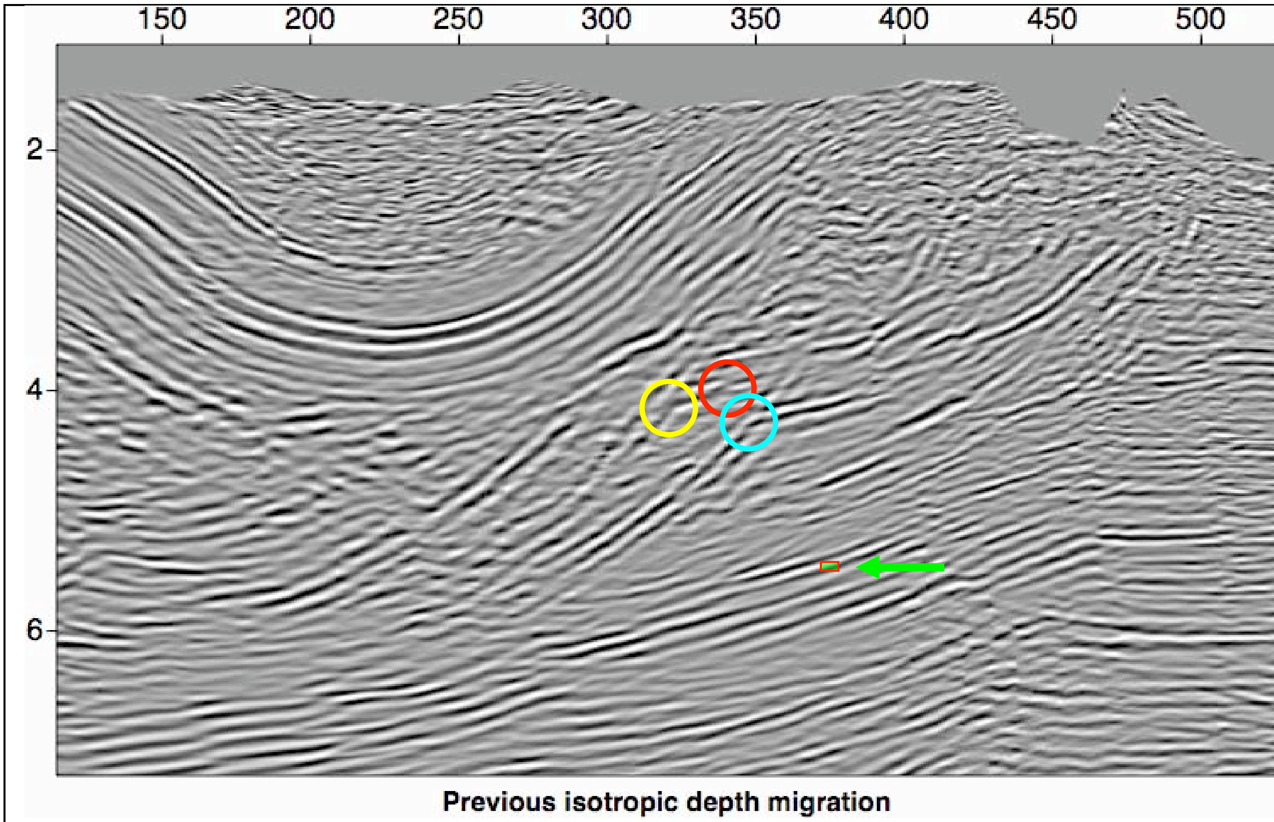

Figure 6. Inline slice from a previous isotropic depth migration project. The green marker represents the position that the well intersected the target horizon. The circles show the position of a fold on a reflector as it appears on the time section (yellow), the isotropic depth section (blue), and the anisotropic depth section (red).

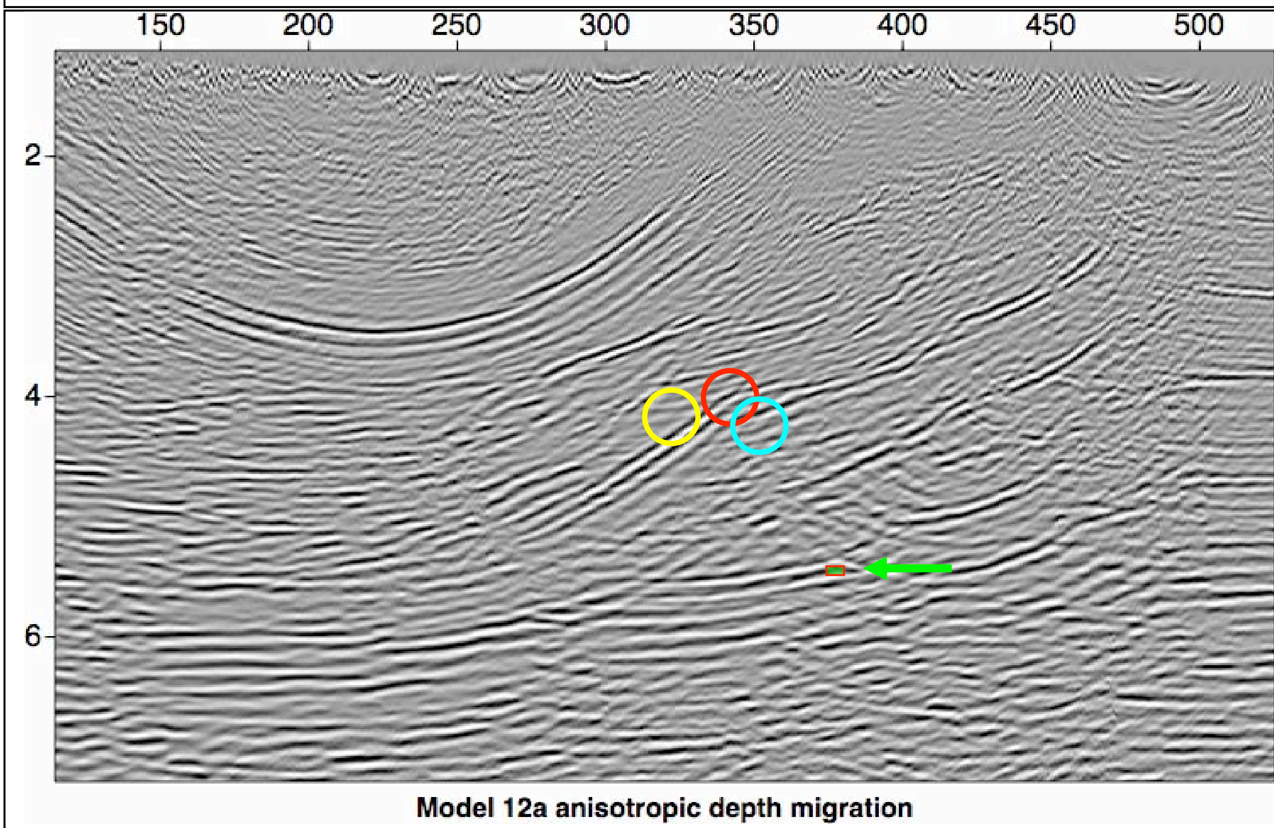

Figure 7. Inline slice from prestack anisotropic depth migration after 12 iterations of model building. The green marker represents the position that the well intersected the target horizon. The circles show the position of a fold on a reflector as it appears on the time section (yellow), the isotropic depth section (blue), and the anisotropic depth section (red).